Atmos. Chem. Phys. Discuss., 12, 17465–17501, 2012
www.atmos-chem-phys-discuss.net/12/17465/2012/
doi:10.5194/acpd-12-17465-2012

Atmospheric Chemistry and Physics Discussions

Modeling South America regional smoke plume: aerosol optical depth variability and shortwave surface forcing

N. E. Rosário[1,2], K. M. Longo[1], S. R. Freitas[1], M. A. Yamasoe[2], and R. M. Fonseca[1]

[1]National Institute for Space Research, Av dos Astronautas, 1.758, Jd. Granja – CEP: 12227-010, São José dos Campos, Brazil
[2]Atmospheric Sciences Department, University of São Paulo, São Paulo, Brazil

Received: 5 June 2012 – Accepted: 19 June 2012 – Published: 17 July 2012

Correspondence to: N. E. Rosário (nilton.rosario@inpe.br)

Published by Copernicus Publications on behalf of the European Geosciences Union.

Abstract

Intra-seasonal variability of smoke aerosol optical depth (AOD) and downwelling solar irradiance at the surface during the 2002 biomass burning season in South America was modeled using the Coupled Chemistry-Aerosol-Tracer Transport model to the Brazilian developments on the Regional Atmospheric Modeling System (CCATT-BRAMS). Measurements of AOD from the AErosol RObotic NETwork (AERONET) and solar irradiance at the surface from the Solar Radiation Network (SolRad-NET) were used to evaluate model results. In general, the major features associated with AOD evolution over the southern part of the Amazon Basin and cerrado ecosystem are captured by the model. The main discrepancies were found for high aerosol loading events. In the northeastern portion of the Amazon Basin the model systematically underestimated AOD. This is likely due to the cloudy nature of the region, preventing accurate detection of the fire spots used in the emission model. Moreover, measured AOD were very often close to background conditions and emissions other than smoke were not considered in the simulation. Therefore, under the background scenario, one would expect the model to underestimate AOD. The issue of high aerosol loading events in the southern part of the Amazon and cerrado is also discussed in the context of emission shortcomings. The Cuiabá cerrado site was the only one where the highest quality AERONET data were unavailable. Thus, lower quality data were used. Root-mean-square-error (RMSE) between the model and observations decreased from 0.48 to 0.17 when extreme AOD events ($AOD_{550\,nm} \geq 1.0$) and Cuiabá were excluded from analysis. Downward surface solar irradiance comparisons also followed similar trends when extremes AOD were excluded. This highlights the need to improve the modelling of the regional smoke plume in order to enhance the accuracy of the radiative energy budget. Aerosol optical model based on the mean intensive properties of smoke from the southern part of the Amazon Basin produced a radiative forcing efficiency (RFE) of $-158\,W\,m^{-2}/AOD_{550\,nm}$ at noon. This value is in between $-154\,W\,m^{-2}/AOD_{550\,nm}$ and $-187\,W\,m^{-2}/AOD_{550\,nm}$, the range obtained when spatial varying optical models were

ACPD
12, 17465–17501, 2012

Modeling South America regional smoke plume

N. E. Rosário et al.

considered. The average 24 h surface forcing over the biomass burning season varied from −55 $W m^{-2}$ close to smoke sources in the southern part of the Amazon Basin and cerrado to −10 $W m^{-2}$ in remote regions of the Southeast Brazilian coast.

1 Introduction

Aerosols direct radiative effect (DRE), which consists of scattering and absorption of solar radiation, plays an important role in Earth's radiative energy budget (Haywood and Boucher, 2000; Menon, 2004; Ramanathan et al., 2001). Despite the advances achieved during the last decades regarding the role of aerosols in Earth's climate processes, the modeling of aerosol DRE in climate models is still a challenging task (Schulz et al., 2006; Forster et al., 2007). Estimates of aerosols global annual mean Direct Radiative Forcing (DRF) diverge considerably between climate models, ranging from +0.04 to −0.41 $W m^{-2}$ (Schulz et al., 2009). The relationship between aerosol optical properties and radiative forcing efficiency, forcing per unit of optical depth, has been pointed out as a key aspect concerning model diversity (Schulz et al., 2006, 2009), particularly for regions dominated by carbonaceous and dust aerosols (Kinne et al., 2006). Over South America in particular, while some models simulated spatial variability in DRF from +2 to −2 $W m^{-2}$, other exhibited lower geographical variation (from −0.2 to −0.4 $W m^{-2}$). Biomass burning is a major source of carbonaceous aerosols to the regional atmosphere, yet observational characterization and model representations of smoke aerosol emission, spatial and temporal variability of abundance and intrinsic optical properties are still uncertain (Kinne et al., 2006; Reid et al., 2005; Longo et al., 2010). Kinne et al. (2006) found biomass burning season in South America to start and to peak too earlier in models used by the AErosol model COMparison experiment (AEROCOM, Textor et al., 2006) when compared with ground based and satellite observation. The study also pointed out that models in general underestimate the strength of the biomass burning season.

ACPD
12, 17465–17501, 2012

The present paper describes results of a modeling effort aiming to simulate the South American regional smoke plume produced during the 2002 biomass burning season. The study was conducted using the Chemistry-Coupled Aerosol and Tracer Transport model to the Brazilian developments on the Regional Atmospheric Modeling System (CCATT-BRAMS, Freitas et al., 2009; Longo et al., 2010, 2012) developed at Brazilian National Institute for Space Research for regional studies of air quality impact on public health, weather forecast and climate processes. The presented results focus on the simulation AOD of the smoke regional plume and the associated surface direct radiative forcing. Downward solar radiation at the surface is a fundamental component in the diurnal cycle of energy budget. The model's ability to correctly simulate AOD field is crucial to an accurate modeling of the solar radiation field. To evaluate the CCATT-BRAMS results, collocated observations of AOD from AErosol RObotic NETwork (AERONET, Holben et al., 1998) sun-photometers and downwelling solar irradiance at the surface from Solar Radiation Network (SolRad-NET, Schafer et al., 2002) pyranometers are used. The paper is divided as follows: Sect. 2 presents a description of the CCATT-BRAMS system with a particular focus on the optical-radiative module. Section 3 describes the experimental data and methods. Results and discussions are presented in Sect. 4. The first results that are presented and discussed are comparisons between model-calculated and observed seasonal variability of aerosol optical depth, followed by evaluation of modeled downwelling solar fluxes at the surface. Next, we discuss radiative forcing efficiencies as parameterized in CCATT–BRAMS based on optical properties models derived from AERONET data. An estimate of RFE from an independent empirical approach based on pyranometer measurements and radiative transfer closure experiment is also presented. Finally, we evaluate the surface radiative forcing induced by the regional smoke plume on 24 h basis and at specific daytimes. Conclusions are presented in Sect. 5.

ACPD
12, 17465–17501, 2012

2 Modeling system description

CCATT-BRAMS consists of a numerical system designed to predict and study emission, deposition and transport of aerosols and other tracers at a regional scale. CCATT is an on-line Eulerian transport model and BRAMS is based on the Regional Atmospheric Modelling System (RAMS, Walko et al., 2000) with specific developments and parameterizations for South America tropical regions. CCATT-BRAMS is fully coupled in order to solve the transport of gaseous compounds and aerosols particles simultaneously with the atmospheric state evolution using exactly the same time-step as well as the dynamics and physical parameterizations. The CCATT module includes gaseous chemistry, photochemistry, scavenging and dry deposition. The resultant 3-D aerosol loading is used as an input to the radiative transfer module in order to simulate aerosols direct and semi-direct radiative effects. Therefore, aerosols impacts on energy budget and atmospheric thermodynamic are considered (Freitas et al., 2009; Longo et al., 2006). Smoke aerosol particles are the focus of the present study. Their emissions were prescribed using the Brazilian Biomass Burning Emission Model (3BEM, Freitas et al., 2005; Longo et al., 2010). The 3BEM smoke particles emission is based on fire pixels counting and burning area database derived from remote-sensing fire products. For detected fire pixels, the mass emitted is obtained combining the amount of above-ground biomass available and the combustion and emission factors for specific species in accordance with the type of vegetation. Fire pixels and burnt area are obtained from several satellite products to minimize missing observation. For products that do not provide estimative of the burning area, a climatological area is assumed. A detailed description of 3BEM model is presented in Longo et al. (2010) and Freitas et al. (2011). For the present study, was considered only emission of carbon monoxide (CO) and smoke fine mode particles, i.e. particles with diameter smaller than 2.5 µm. In areas heavily affected by biomass burning, in the southern region of the Amazon Basin and the cerrado ecosystem, fine mode aerosols contributes on average to, respectively, 90 % and 85 % of the aerosol optical depth in the visible spectrum (Rosário,

ACPD
12, 17465–17501, 2012

2011a). Moreover, fine mode particles dominate the regional smoke plume intensive radiative properties (Reid et al., 2005). Although only smoke emission was considered in the present study, it is worth to mention that CCATT-BRAMS system is able to treat distinct aerosol types. CCATT-BRAMS was configured and ran within two domains (Fig. 1). The first consisted of a larger domain with 140 km horizontal resolution covering South America and Africa aiming to capture inflow of smoke from Africa and transport of South America smoke to remote areas of the southwestern portion of the Atlantic Ocean. The second, a nested grid, consisted of a smaller domain covering only South America and with a horizontal resolution of 35 km. For both domains 42 vertical levels were included with vertical resolution varying from 150 m in the lower troposphere to a maximum of 850 m in the upper troposphere. Atmospheric initial and boundary conditions were assimilated from the analysis of the global model of the Brazilian Center for Weather Forecasting and Climate Studies using RAMS assimilation scheme.

2.1 CCATT-BRAMS optical-radiative module

The CCATT-BRAMS optical-radiative module is based on a modified version of the Community Aerosol and Radiation Model for Atmosphere (CARMA, Toon et al., 1988; Colarco et al., 2002). The original CARMA version considered simultaneously an aerosol microphysics scheme and two-stream radiative transfer module for both spectral regions solar and terrestrial. Major standard microphysical processes, such as coagulation, condensational growth and particle sedimentation were included. Aerosols size distribution was prescribed using several bins and including different chemical elements. Aerosols particles were treated as spherical and internal mixed. Mie calculations were performed simultaneously with radiative transfer in order to provide aerosols extinction, scattering and absorption spectral coefficients. The elaborated and complex scheme of original CARMA turned out to be expensive and prohibitive to run in an operational mode. Therefore the aerosols microphysic scheme was simplified while the radiative transfer module was kept with minor modifications. The major modification

Discussion Paper | Discussion Paper | Discussion Paper | Discussion Paper |
ACPD
12, 17465–17501, 2012
Modeling South America regional smoke plume
N. E. Rosário et al.

from the original version refers to the prescription of aerosol intensive optical properties, specifically extinction efficiency ($Q_{ext,\lambda}$), single scattering albedo ($\omega_{o\lambda}$) and asymmetry parameter (g_λ). Currently these parameters are obtained previously from off-line Mie calculations unlike of the original on-line calculations. Prior prescription of smoke optical properties in CCATT-BRAMS was based on the study of Procopio et al. (2003). Climatological size distribution and complex refractive index from two AERONET sites in the southern of the Amazon Basin were used as input to an off-line Mie code to calculate the spectral optical properties required by CARMA. Using this approach Procópio et al. (2003) developed a set of dynamic aerosol optical models defined by aerosol optical depth. Rosario et al. (2011a) using several AERONET sites and longer time-series extended the development of aerosol optical properties aiming to represent the spatial variability across major biomass burning areas of South America. Figure 2 shows the typical spectral dependence of optical properties for the sites in these areas, specifically, southern and north-eastern of the Amazon Basin and cerrado. Main features are the higher absorption of aerosols particles from cerrado, the consistency between the sites in the southern of the Amazon Basin and the difference between the two sites in the northeast of the Amazon. The reason of this difference is no yet well understood. The higher absorption of cerrado smoke aerosol has been associated with the dominance of flaming phase combustion (Yamasoe et al., 1998; Dubovik et al., 2002). These spectral optical models were calculated using average size distribution and complex refractive index of aerosols in a Mie code (Wiscombe, 1980). The spacialization of the optical models in CCATT-BRAMS was performed based on the concept of anisotropic areas of influence described in Hoelzemann et al. (2009). Elsewhere in the model domain not covered by the areas of influence was adopted a reference optical model. The reference model was obtained using as input to Mie calculations the average of size distribution and complex refractive index from sites located in the southern of the Amazon Basin (Rio Branco, Abracos Hill and Alta Floresta). Smoke from the southern region of the Amazon Basin is the main contributor of biomass burning aerosols particles to remote regions of South America (Freitas et al., 2005; Longo

ACPD
12, 17465–17501, 2012

et al., 2009). Spectral aerosol optical depth (AOD_λ) is calculated based on the aerosol loading field provided by CCATT-BRAMS transport module and the spectral extinction efficiency factor stored in look-up-tables. The AOD_λ along with $\varpi_{o\lambda}$ and g_λ are used as input in CARMA radiative transfer code in order to simulate the aerosol direct radiative effect. CARMA two-stream radiative transfer is treated by dividing solar and infrared radiation into 32 and 19 wavelength narrow-bands, respectively. Gaseous absorption and emission are calculated using an exponential sum formulation (Toon et al., 1989). All major atmosphere radiative active constituents, water vapour, ozone, carbon dioxide and oxygen are taken into account. Cloud optical properties are parameterized accordingly to Sun and Shine (1994) and Savijarvi et al. (1997) using liquid and ice particle content provided by CCATT-BRAMS cloud microphysical module. Aerosol indirect effects were not considered in the present study, therefore, the aerosol radiative impacts analyzed are strictly associated with the direct effect. CCATT-BRAMS was ran three times. First unplugging aerosols direct radiative effect. For the second run aerosols effect was turned on considering static optical properties based on the reference optic model (Fig. 2). The third run also included aerosols radiative effect, however was prescribed spatial varying optical properties as described above. The impacts of aerosol direct radiative effect were evaluated analyzing differences between run including and excluding aerosol radiative effects. All results analyzed in this study are related to the smaller domain.

3 Experimental data and methods

The geographical locations of the analyzed AERONET sites are depicted in Fig. 1 using as background the mean field of $AOD_{550\,nm}$ during the 2002 biomass burning season from the Moderate Resolution Imaging Spectroradiometer (MODIS) aboard TERRA satellite. Details regarding location, dominant ecosystems and experimental data from each site are provided in Table 1. Observed aerosol optical depth data were taken from AERONET database, and measured broadband downwelling solar radiation at the

ACPD
12, 17465–17501, 2012

surface from SolRad-Net. Only the highest quality measurements (level 2.0) from both networks were considered, which are pre- and post-field calibrated. The exception was the Cuiabá site where aerosol optical properties from level 2.0 are unavailable, thus data from level 1.5 was used. AERONET's aerosol optical depth uncertainty is stated to vary from 0.01 to 0.02 (Eck et al., 1999) and pyranometers absolute uncertainty range between 2 % and 3 % (Schafer et al., 2002). The comparative analysis of AOD between AERONET and CCATT-BRAMS was performed based on daily averages, while surface irradiance were compared at specific times 12:00, 15:00 and 18:00 UTC. Observed irradiances were averaged over 30 min intervals centered at the mentioned times. Samples with large temporal variations in the solar irradiance at surface level were assumed to be cloud contaminated, and were therefore excluded. Adopted additional criteria to perform cloud screening are further described in Rosário et al. (2011b). Cloud fractions in the Amazon Basin is considerably high even during the dry season (Asner et al., 2001). This is very likely to explain the scarcity of clear sky conditions over a large period of time. For both AOD and surface solar irradiance, model results were collocated with the experimental stations assuming a window-size of 90 × 90 km centered at each site. Additionally, downward solar irradiance at the surface was calculated for Rio Branco, Abracos Hill, Alta Floresta and Cuiabá using AOD and column water vapour (CWV) from AERONET as input to the column radiative transfer code Santa Barbara DISORT Atmospheric Radiative Transfer (SBDART, Ricchiazzi et al., 1998). For cloudless conditions and at a given sun geometry, AOD and CWV variation are expected to explain most of variability in downwelling solar irradiance at the surface. SBDART is an efficient column code for closure experiments that has been used to study radiative transfer in smoky environment in South America (Procopio et al., 2003, 2004; Rosario et al., 2011b). Rosário et al. (2011b) were able to reproduce the observed variability of solar irradiance when instantaneous AOD and CWV from AERONET were prescribed as inputs. The SBDART results were included in the comparison analysis between CCATT-BRAMS outputs and pyranometers measurements. Mean surface radiative forcing on 24 h basis and at specific daytimes was estimated averaging over the biomass burning

ACPD
12, 17465–17501, 2012

season instantaneous difference between modeled downward surface solar irradiance including and excluding smoke aerosol radiative effect. The dependence of radiative forcing efficiency on the adopted optical model was evaluated accordingly to Hansell et al. (2003) and Stone et al. (2011) methodology. The method is based on linear fitting of aerosol optical depth versus the difference between downwelling solar irradiance at the surface considering and neglecting aerosol direct radiative effect. The slope of the linear fitting provides an estimate of RFE. An independent empirical RFE was also calculated based on a synergy between pyranometer, sunphotometer and SBDART. Pyranometers measurements were defined to represent downwelling solar irradiance at the surface under the influence of the aerosol radiative effect. Collocated column water vapour from sunphotometer, ozone from the Total Ozone Mapping Spectrometer (TOMS) and broadband surface albedo taken from the observational study of Berbet and Costa (2003) were used as input into the SBDART radiative transfer code to simulate the solar irradiance at the surface without aerosol influence. The independent empirical RFE was obtained as the slope from the linear fitting of the difference between measured irradiance at the surface and aerosol free irradiance calculated as a function of observed AOD. This case is assumed free of assumptions on aerosol optical properties.

4 Results

4.1 Aerosol optical depth and solar flux comparisons

A major feature of AOD across the biomass burning season is its high spatial and time variability induced by a set of complex processes, such as random and intermittent emissions sources, atmospheric transport and removal processes and variation of particles' intrinsic properties due to aging and mixing processes (Eck et al., 2009; Reid et al., 2005). Figure 3 compares model-calculated and observed intra-seasonal variability of $AOD_{550\,nm}$ over distinct AERONET sites. In general, a significant agreement

ACPD
12, 17465–17501, 2012

between model and observations is seen concerning the evolution of aerosol optical depth for the sites in southern of the Amazon Basin and cerrado. This suggests that the model is able to capture major features of the chain of processes mentioned above in those regions. Nonetheless, divergences between model results and AERONET can be observed. Particularly over the sites in the north-eastern of the Amazon Basin (Belterra and Balbina). Model is systematically lower than observation. As can be seen in Fig. 1, the north-eastern region is marginally affected by the regional smoke plume. AOD peaks in November mostly associated with local emission. The systematic discrepancy between model and AERONET is likely to be linked to two aspects. The cloudy nature of Balbina and Belterra region, which might prevent accurate remote sensing of fire spots and the dominance of natural AOD conditions ($AOD_{550\,nm} \leq 0.2$). In the present study only fire emission was considered. Therefore, under background scenario one would expect model to underestimated AOD. Hereinafter, analysis focused on southern of the Amazon Basin and cerrado sites. These are located inside the core of the regional smoke plume. Regarding these sites the critical aspect seen in the comparison is the model struggling to capture high AOD events, especially over Alta Floresta and Cuiabá (Fig. 4). Table 2 shows statistical parameters of the AOD comparison. Statistical analysis was performed dividing data in three sets: (1) all stations (Rio Branco, Abracos Hill, Alta Floresta and Cuiabá), (2) excluding Cuiabá and keeping all the other sites and (3) for each station individually. The Cuiabá station was excluded because it is the only one for which AERONET post-field calibrated data was not available. Table 2 also shows statistic excluding extreme events by defining a threshold ($AOD_{550\,nm} \leq 1.0$). Extreme AOD events represent roughly 20 % of the dataset. It is clear that the worse (RMSE = 0.48) and the best (RMSE = 0.17) comparison between model outputs and observations are obtained when the Cuiabá site and extreme events are included and excluded in the analysis, respectively. Unlike sunphotometer, due to relatively coarse grid resolution, the model is not expected to capture highly dense and localized plumes. However, the persistence of divergences between model and observation during large time period suggests that modeling aspects, beyond grid

ACPD
12, 17465–17501, 2012

characteristic, may play an important role in the observed differences. Given the magnitude of the differences, variability in particles intensive optical properties are unlikely to play a major role. It is more plausible that emissions are the critical aspect. Fire focus omission or misrepresentation can induce important errors in the emission and consequently in aerosol loading field. Image-acquisition geometry and cloud coverage conditions have been pointed-out as important issues in this matter (Schroeder et al., 2005, 2008). By comparing satellite fire focus retrieval with aircraft observation over the southwest of the Amazon Basin, Pantoja and Brown (2007) showed that divergence between the two sources of data were consistently associated with satellite fire focus omission. Emission based on remote sensing of fire brought large improvements to the smoke modeling in South America when compared with conventional database (Longo et al., 2010). However, the spatial and temporal scale of fire occurrence might still impose a considerable detection error. Thus, it is very likely that emission issues are playing a major role in the observed divergence between model and observation. Figures 5 and 6 show comparisons between model-calculated and observed solar irradiance at surface under cloud-free conditions. Observational data is scarce during the afternoon (15:00 UTC, 18:00 UTC) mainly due to the increase in cloudiness. Consequently, AOD signature on surface solar irradiance is better identified looking at morning data (12:00 UTC). The SBDART estimation of solar irradiance at surface using AOD and column water vapour from AERONET sunphotometer as input is also plotted. Main trends in solar irradiance at surface are in general well captured by the model. This is an outcome of the model ability to predict the major features of AOD variability. Nevertheless, non negligible discrepancies are still occurring. Figure 7 shows differences between measured and modeled solar irradiance as a function of collocated differences between observed and modeled AOD. The linear relationship highlights the dominance of aerosol optical depth as major source of uncertainty when it comes to the modeling of solar irradiance at the surface. Table 3 shows statistics of the comparison between model and pyranometers. Yet again, the best scenario (RMSE = 31 $\mathrm{W\,m^{-2}}$) occurs when Cuiabá site and extreme AOD events are excluded from the analysis.

ACPD
12, 17465–17501, 2012

When all data were considered the agreement between the model and the observations decreased (RMSE = 45 W m^{-2}). The Cuiabá site performed worse for irradiance intercomparison than the other sites, data not shown. The larger positive discrepancies observed may be related to eventual cloud contamination. In spite of the application of cloud screening procedure to both pyranometer and sun photometer dataset. However, they are not expected to alter significantly the general assessments of the present analysis. In summary, the comparisons show that CCATT-BRAMS was able to reproduce the main features of the AOD field associated with the regional smoke plume, and to capture its seasonal variability and impacts on the downwelling solar energy at the surface. Major difficulty seems to be related to extreme smoke events ($AOD_{550\,nm} > 1.0$). Although these events in general represent less than 20 % of the total AERONET samples from the direct sun inversion, their impacts are significant. Therefore the aspects behind this model struggling need to be addressed. A conclusive analysis of the impact of satellite scan geometry and clouds on emission modelling need to be performed. Apparently, the days in the present study with major deviations coincided with smoky area being imaged under larger scan angles (W. Schroeder, personal communication, 2004).

4.2 Radiative forcing efficiency and surface forcing

Radiative forcing efficiency (RFE) is a metric of the sensitivity of the aerosol radiative forcing to aerosol types and is primarily controlled by aerosol intrinsic properties. Figure 8 shows regression plots of AOD versus differences between solar irradiance at the surface neglecting and considering aerosol direct radiative effects. The results are shown for noontime when instantaneous surface forcing is expected to be high. The slopes represent estimates of mean RFE. Regressions are presented for aerosol direct radiative effect modeled using the reference optical model and optical models of Rio Branco, Abracos Hill, Alta Floresta, Cuiabá previously shown in Fig. 2. For the sites inside the Amazon Basin the RFE varied between −154 and −163 W m^{-2}/$AOD_{550\,nm}$ range. The RFE for the reference optical model (−158 W m^{-2}/$AOD_{550\,nm}$) is consistently

ACPD
12, 17465–17501, 2012

in the middle of the range. An independent empirical estimate based on pyranometers and sunphotometer measurements for the southern of the Amazon Basin is also shown ($-141\,\mathrm{W\,m^{-2}}/\mathrm{AOD}_{550\,\mathrm{nm}}$). Smoke aerosol in cerrado (Cuiabá) has higher RFE ($-187\,\mathrm{W\,m^{-2}}/\mathrm{AOD}_{550\,\mathrm{nm}}$) mainly due to its larger absorption. The obtained RFE are compared with values found in the literature (Table 4). Concerning the southern region of the Amazon Basin, the obtained RFE are higher than empirical value estimated by Schafer et al. (2002) for Abracos Hill and Alta Floresta sites but consistent with the overall RFE variability. Regarding the difference between the empiricals RFE and those obtained using climatological optical model, one can argue that is likely due to the fact that the former has been obtained for particular years. Figure 9 shows 24 h smoke surface forcing averaged over the biomass burning season. Results are presented for both model runs considering static and varying optical properties models. As expected, major differences between both approaches are seen downwind of the Amazon Basin. On average single scattering albedo inverted by AERONET sites downwind are lower than values retrieved inside the southern region of the Amazon Basin. The spatial range of daily mean surface forcing in the southern of the Amazon Basin (-35 to $-50\,\mathrm{W\,m^{-2}}$) is consistent with Procópio et al. (2004) results (-34.5 to $-48\,\mathrm{W\,m^{-2}}$). Regionally, the smoke surface forcing varies from $-55\,\mathrm{W\,m^{-2}}$, in areas heavily affected by biomass burning emission, to $-10\,\mathrm{W\,m^{-2}}$ near the Brazilian southeastern coast. In the northwestern portion of the Amazon Basin the surface forcing is also $-10\,\mathrm{W\,m^{-2}}$. Figure 10 shows mean surface forcing at specific times (12:00, 15:00, 18:00 and 21:00 UTC) in order to highlight the daytime cycle. Maximum perturbation occurs at noontime (15:00 UTC) and it is around $-100\,\mathrm{W\,m^{-2}}$ in areas close to the emission sources. The diurnal cycle of the impact on lower troposphere net radiative heating profile is shown (Fig. 11) through a cross section at longitude 57° W, all along the South American continent, from clean areas in the northern of South America, crossing biomass burning region in central regions, and up to the northern region of Argentina at 35° S. The net effect is essentially a warming of the atmosphere. As expected, higher impacts are observed at noontime when larger amount of solar energy is available. Net radiative heating rate when smoke is included can be twice that of aerosol free case. The net impact of both solar energy reduction at the surface and enhancement of radiative heating rate induced by the regional smoke on the South American climate is still uncertain and subject of research. Accurate modeling of the spatio-temporal distribution of the regional smoke loading and its intrinsic radiative properties remain a challenging task. Results of the present study indicated that the CCATT-BRAMS model is able to simulate consistently major features of AOD variability related to the regional smoke plume as well as the impact on downward shortwave radiation at the surface. However, important deviations from observations are still occurring. Ongoing researches are expected to tackle these issues.

5 Final remarks

The present paper describes a modeling effort to simulate the aerosol optical depth of the regional smoke produced during the biomass burning season of 2002 and the associated surface direct radiative forcing in the Amazon Basin and cerrado ecosystem. The CCATT-BRAMS model developed at National Institute for Spatial Research for air quality and climate studies was used. CCATT-BRAMS is a fully coupled on-line model, which allows feedbacks between aerosol radiative effect and other atmospheric processes. Generally, comparisons between model-calculated variability of AOD and data from AERONET showed significant agreement. The model was able to capture the major features of AOD across the burning season over most of analyzed AERONET sites. The main shortcomings were the underestimation of AOD in the north eastern region of the Amazon Basin and the model difficulty to capture extreme AOD events ($AOD_{550\,nm} > 1.0$). The latter struggle was particularly evident in the cerrado region and the transition areas from primary forest to cerrado. Accordingly to AERONET direct sun inversion extreme events represent roughly 20 % of conditions observed during the biomass burning season, however their radiative impacts are huge. They can reduce solar irradiance at the surface by values up to 300 W m^{-2}. The main suspicion

ACPD
12, 17465–17501, 2012

of the model difficulty to capture these events is related to emission estimation. The fire focus omission very likely to explains this deficiency. The root-mean-square error (RMSE) between modeled and observed AOD decreases from 0.48 to 0.17 when extreme AOD events and the Cuiabá site were excluded from the analysis. A similar trend was observed when the modeled downwelling solar irradiance at the surface was compared with pyranometers measurements. Better agreement was achieved between CCATT-BRAMS and observations when data was restricted to irradiance measured under $AOD_{550\,nm}$ lower than 1.0. Ongoing modeling simulations and planned future field experiments are expected to allow more conclusive analysis on this respect.

Radiative forcing efficiency (RFE) obtained using space varying optical models was compared with RFE using a static optical model prescription. The static model consisted of typical optical properties of smoke aerosol produced in the southern of the Amazon Basin. Major impacts on surface forcing were observed downwind of the Amazon Basin where smoke aerosol plumes are on average more absorbing. Mean 24 h surface forcing induced by the regional smoke plume varied from $-55\,W\,m^{-2}$ to $-10\,W\,m^{-2}$, from biomass burning areas to remote regions in the southeast of Brazil and in the northwest portion of the Amazon Basin. In areas close to the emission sources the enhancement of the net radiative heating rate by the regional smoke was as much as double the aerosol free condition. Our results pointed out the ability of CCATT-BRAMS to simulate major spatio-temporal features of aerosol optical depth field associated with South American regional smoke, despite the simplified aerosol microphysics adopted. The observed performance is a consequence of recent improvements of regional smoke dynamics in the model, particularly emission regionalization (Longo et al., 2010) and the inclusion of sub-grid scale plume rise from vegetation fires (Freitas et al., 2007). Nevertheless, shortcomings were also observed and emission is still a critical aspect and a matter of continuing research. Ongoing developments on CCATT-BRAMS and its emission module are expected to improve the modeling of regional aerosol chemistry in South America.

ACPD
12, 17465–17501, 2012

Acknowledgements. The first author wishes to thank CNPq (Conselho Nacional de Desenvolvimento Científico e Tecnológico) for the financial support (processes 140559/2007-8; 201177/2009-9). Additional thanks to AERONET, SolRad-Net teams for making available the data used in this study. M. Yamasoe acknowledges FAPESP (Fundação de Amparo à Pesquisa do Estado de São Paulo), process number 06-56550-5 and CAPES/PROEX (Coordenação de Aperfeiçoamento de Pessoal de Nível Superior/Programa de Excelência Acadêmica).

References

Asner, G. P.: Cloud cover in Landsat observations of the Brazilian Amazon, Int. J. Remote Sens., 22, 3855–3862, 10.1080/01431160010006926, 2001.

Berbet, M. L. C. and Costa, M. H.: Climate change after tropical deforestation: seasonal variability of surface albedo and its effects on precipitation change, J. Climate, 16, 2099–2104, doi:10.1175/1520-0442(2003)016<2099:ccatds>2.0.co;2, 2003.

Colarco, P. R., Toon, O. B., Torres, O., and Rasch, P. J.: Determining the UV imaginary index of refraction of Saharan dust particles from total ozone mapping spectrometer data using a three-dimensional model of dust transport, J. Geophys. Res., 107, 4289, doi:10.1029/2001jd000903, 2002.

Dubovik, O., Holben, B., Eck, T. F., Smirnov, A., Kaufman, Y. J., King, M. D., Tanré, D., and Slutsker, I.: Variability of absorption and optical properties of key aerosol types observed in worldwide locations, J. Atmos. Sci., 59, 590–608, doi:10.1175/1520-0469(2002)059<0590:voaaop>2.0.co;2, 2002.

Eck, T. F., Holben, B. N., Reid, J. S., Dubovik, O., Smirnov, A., O'Neill, N. T., Slutsker, I., and Kinne, S.: Wavelength dependence of the optical depth of biomass burning, urban, and desert dust aerosols, J. Geophys. Res., 104, 31333–31349, doi:10.1029/1999jd900923, 1999.

Eck, T. F., Holben, B. N., Reid, J. S., Sinyuk, A., Hyer, E. J., O'Neill, N. T., Shaw, G. E., Vande Castle, J. R., Chapin, F. S., Dubovik, O., Smirnov, A., Vermote, E., Schafer, J. S., Giles, D., Slutsker, I., Sorokine, M., and Newcomb, W. W.: Optical properties of boreal region biomass burning aerosols in central Alaska and seasonal variation of aerosol optical depth at an Arctic coastal site, J. Geophys. Res., 114, D11201, doi:10.1029/2008jd010870, 2009.

Freitas, S. R., Longo, K. M., Chatfield, R., Latham, D., Silva Dias, M. A. F., Andreae, M. O., Prins, E., Santos, J. C., Gielow, R., and Carvalho Jr., J. A.: Including the sub-grid scale plume rise of vegetation fires in low resolution atmospheric transport models, Atmos. Chem. Phys., 7, 3385–3398, doi:10.5194/acp-7-3385-2007, 2007.

Freitas, S. R., Longo, K. M., Silva Dias, M. A. F., Chatfield, R., Silva Dias, P., Artaxo, P., Andreae, M. O., Grell, G., Rodrigues, L. F., Fazenda, A., and Panetta, J.: The Coupled Aerosol and Tracer Transport model to the Brazilian developments on the Regional Atmospheric Modeling System (CATT-BRAMS) – Part 1: Model description and evaluation, Atmos. Chem. Phys., 9, 2843–2861, doi:10.5194/acp-9-2843-2009, 2009.

Freitas, S. R., Longo, K. M., Alonso, M. F., Pirre, M., Marecal, V., Grell, G., Stockler, R., Mello, R. F., and Sánchez Gácita, M.: PREP-CHEM-SRC – 1.0: a preprocessor of trace gas and aerosol emission fields for regional and global atmospheric chemistry models, Geosci. Model Dev., 4, 419–433, doi:10.5194/gmd-4-419-2011, 2011.

Forster, P., Ramaswamy, V., Artaxo, P., Berntsen, T., Betts, R., Fahey, D. W., Haywood, J., Lean, J., Lowe, D. C., Myhre, G., Nganga, J., Prinn, R., Raga, G., Schulz, M., and Van Dorland, R.: Changes in atmospheric constituents and in radiative forcing, in: Climate Change 2007: The Physical Science Basis, Contribution of Working Group I to the Fourth Assessment Report of the Intergovernmental Panel on Climate Change, edited by: Solomon, S., Qin, D., Manning, M., Chen, Z., Marquis, M., Averyt, K. B., Tignor, M., and Miller, H. L., Cambridge University Press, Cambridge, UK and New York, NY, USA, 2007.

Hansell, R. A., Tsay, S.-C., Ji, Q., Liou, K. N., and Ou, S.-C.: Surface aerosol radiative forcing derived from collocated ground-based radiometric observations during PRIDE, SAFARI, and ACE-Asia, Appl. Optics, 42, 5533–5544, 2003.

Haywood, J. and Boucher, O.: Estimates of the direct and indirect radiative forcing due to tropospheric aerosols: a review, Rev. Geophys., 38, 513–543, doi:10.1029/1999rg000078, 2000.

Hoelzemann, J. J., Longo, K. M., Fonseca, R. M., do Rosário, N. M. E., Elbern, H., Freitas, S. R., and Pires, C.: Regional representativity of AERONET observation sites during the biomass burning season in South America determined by correlation studies with MODIS Aerosol Optical Depth, J. Geophys. Res., 114, D13301, doi:10.1029/2008jd010369, 2009.

Holben, B. N., Eck, T. F., Slutsker, I., Tanré, D., Buis, J. P., Setzer, A., Vermote, E., Reagan, J. A., Kaufman, Y. J., Nakajima, T., Lavenu, F., Jankowiak, I., and Smirnov, A.: AERONET – a federated instrument network and data archive for aerosol characterization, Remote Sens. Environ., 66, 1–16, doi:10.1016/s0034-4257(98)00031-5, 1998.

ACPD
12, 17465–17501, 2012

Kinne, S., Schulz, M., Textor, C., Guibert, S., Balkanski, Y., Bauer, S. E., Berntsen, T., Berglen, T. F., Boucher, O., Chin, M., Collins, W., Dentener, F., Diehl, T., Easter, R., Feichter, J., Fillmore, D., Ghan, S., Ginoux, P., Gong, S., Grini, A., Hendricks, J., Herzog, M., Horowitz, L., Isaksen, I., Iversen, T., Kirkevåg, A., Kloster, S., Koch, D., Kristjansson, J. E., Krol, M., Lauer, A., Lamarque, J. F., Lesins, G., Liu, X., Lohmann, U., Montanaro, V., Myhre, G., Penner, J., Pitari, G., Reddy, S., Seland, O., Stier, P., Takemura, T., and Tie, X.: An AeroCom initial assessment – optical properties in aerosol component modules of global models, Atmos. Chem. Phys., 6, 1815–1834, doi:10.5194/acp-6-1815-2006, 2006.

Longo, K. M., Freitas, S. R., Dias, M. A. S., and Dias, P. L. S.: Numerical modelling of the biomass-burning aerosol direct radiative effects on the thermodynamics structure of the atmosphere and convective precipitation, in: International Conference on Southern Hemisphere Meteorology and Oceanography (ICSHMO), 8, 2006, Foz do Iguaçu, Proceedings, 283–289, 2006.

Longo, K. M., Freitas, S. R., Andreae, M. O., Yokelson, R., and Artaxo, P.: Biomass burning in Amazonia: emissions, long-range transport of smoke and its regional and remote impacts, in: Amazonia and Global Change, Geophys. Monogr. Ser., AGU, Washington, DC, 207–232, 2009.

Longo, K. M., Freitas, S. R., Andreae, M. O., Setzer, A., Prins, E., and Artaxo, P.: The Coupled Aerosol and Tracer Transport model to the Brazilian developments on the Regional Atmospheric Modeling System (CATT-BRAMS) – Part 2: Model sensitivity to the biomass burning inventories, Atmos. Chem. Phys., 10, 5785–5795, doi:10.5194/acp-10-5785-2010, 2010.

Longo, K. M., Freitas, S. R., Pirre, M., Marécal, V., Rodrigues, L. F., Alonso, M. F., Rosário, N., Mello, R., Moreira, D., Sanches-Gacita, M., Pereira, G. R, and Stockler, R.: The Chemistry-CATT BRAMS model: a new efficient tool for atmospheric chemistry studies at local and regional scales, Geosci. Model Dev. Discuss., submitted, 2012.

Menon, S.: Current uncertainties in assessing aerosol effects on climate, Annu. Rev. Env. Resour., 29, 1–30, doi:10.1146/annurev.energy.29.063003.132549, 2004.

Pantoja, N. V. and Brown, I. F.: Acurácia dos sensores AVHRR, GOES e MODIS na detecção de incêndios florestais e queimadas a partir de observações aéreas no estado do Acre, Brazil, paper presented at the XIII Symposium of Remote Sensing, Florianópolis, Brazil, 21–26 April 2007, INPE, 4501–4508, 2007 (in Portuguese).

ACPD
12, 17465–17501, 2012

Procopio, A. S., Remer, L. A., Artaxo, P., Kaufman, Y. J., and Holben, B. N.: Modeled spectral optical properties for smoke aerosols in Amazonia, Geophys. Res. Lett., 30, 2265, doi:10.1029/2003gl018063, 2003.

Procopio, A. S., Artaxo, P., Kaufman, Y. J., Remer, L. A., Schafer, J. S., and Holben, B. N.: Multiyear analysis of amazonian biomass burning smoke radiative forcing of climate, Geophys. Res. Lett., 31, L03108, doi:10.1029/2003gl018646, 2004.

Ramanathan, V., Crutzen, P. J., Kiehl, J. T., and Rosenfeld, D.: Aerosols, climate, and the hydrological cycle, Science, 294, 2119–2124, doi:10.1126/science.1064034, 2001.

Reid, J. S., Eck, T. F., Christopher, S. A., Koppmann, R., Dubovik, O., Eleuterio, D. P., Holben, B. N., Reid, E. A., and Zhang, J.: A review of biomass burning emissions part III: intensive optical properties of biomass burning particles, Atmos. Chem. Phys., 5, 827–849, doi10.5194/acp-5-827-2005, 2005.

Ricchiazzi, P., Yang, S., Gautier, C., and Sowle, D.: SBDART: a research and teaching software tool for plane-parallel radiative transfer in the earth's atmosphere, B. Am. Meteorol. Soc., 79, 2101–2114, doi:10.1175/1520-0477(1998)079<2101:sarats>2.0.co;2, 1998.

Rosário, N. M. E.: Variability of aerosol optical properties over South America and the impacts of direct radiative effect of aerosols from biomass burning, Ph.D. thesis, Institute of Astronomy, Geophysics and Atmospheric Sciences, University of São Paulo, São Paulo, 2011a (in Portuguese).

Rosário, N. E., Yamasoe, M. A., Brindley, H., Eck, T. F., and Schafer, J.: Downwelling solar irradiance in the biomass burning region of the Southern Amazon: dependence on aerosol intensive optical properties and role of water vapor, J. Geophys. Res., 116, D18304, doi:10.1029/2011jd015956, 2011b.

Savijärvi, H., Arola, A., and Räisänen, P.: Short-wave optical properties of precipitating water clouds, Q. J. Roy. Meteor. Soc., 123, 883–899, doi:10.1002/qj.49712354005, 1997.

Schafer, J. S., Eck, T. F., Holben, B. N., Artaxo, P., Yamasoe, M. A., and Procopio, A. S.: Observed reductions of total solar irradiance by biomass-burning aerosols in the Brazilian Amazon and Zambian Savanna, Geophys. Res. Lett., 29, 1823, doi:10.1029/2001gl014309, 2002.

Schroeder, W., Morisette, J. T., Csiszar, I., Giglio, L., Morton, D., and Justice, C. O.: Characterizing vegetation fire dynamics in Brazil through multisatellite data: common trends and practical issues, Earth Interact., 9, 1–26, doi:10.1175/ei120.1, 2005.

ACPD

12, 17465–17501, 2012

Schroeder, W., Prins, E., Giglio, L., Csiszar, I., Schmidt, C., Morisette, J., and Morton, D.: Validation of GOES and MODIS active fire detection products using ASTER and ETM+ data, Remote Sens. Environ., 112, 2711–2726, doi:10.1016/j.rse.2008.01.005, 2008.

Schulz, M., Textor, C., Kinne, S., Balkanski, Y., Bauer, S., Berntsen, T., Berglen, T., Boucher, O., Dentener, F., Guibert, S., Isaksen, I. S. A., Iversen, T., Koch, D., Kirkevåg, A., Liu, X., Montanaro, V., Myhre, G., Penner, J. E., Pitari, G., Reddy, S., Seland,Ø., Stier, P., and Takemura, T.: Radiative forcing by aerosols as derived from the AeroCom present-day and pre-industrial simulations, Atmos. Chem. Phys., 6, 5225–5246, doi:10.5194/acp-6-5225-2006, 2006.

Schulz, M., Chin, M., and Kinne S.: The Aerosol Model Comparison Project, AeroCom, Phase II: Clearing Up Diversity, IGAC Newsletter, No 41, available at: http://www.igacproject.org/sites/all/themes/bluemasters/images/NewsletterArchives/Issue_41_May_2009.pdf, May 2009.

Stone, R. S., Augustine, J. A., Dutton, E. G., O'Neill, N. T., and Saha, A.: Empirical determinations of the longwave and shortwave radiative forcing efficiencies of wildfire smoke, J. Geophys. Res., 116, D12207, doi:10.1029/2010jd015471, 2011.

Sun, Z. and Shine, K. P.: Studies of the radiative properties of ice and mixed-phase clouds, Q. J. Roy. Meteor. Soc., 120, 111–137, doi:10.1002/qj.49712051508, 1994.

Textor, C., Schulz, M., Guibert, S., Kinne, S., Balkanski, Y., Bauer, S., Berntsen, T., Berglen, T., Boucher, O., Chin, M., Dentener, F., Diehl, T., Feichter, J., Fillmore, D., Ginoux, P., Gong, S., Grini, A., Hendricks, J., Horowitz, L., Huang, P., Isaksen, I. S. A., Iversen, T., Kloster, S., Koch, D., Kirkevåg, A., Kristjansson, J. E., Krol, M., Lauer, A., Lamarque, J. F., Liu, X., Montanaro, V., Myhre, G., Penner, J. E., Pitari, G., Reddy, M. S., Seland,Ø., Stier, P., Takemura, T., and Tie, X.: The effect of harmonized emissions on aerosol properties in global models – an AeroCom experiment, Atmos. Chem. Phys., 7, 4489–4501, doi:10.5194/acp-7-4489-2007, 2007.

Toon, O. B., Turco, R. P., Westphal, D., Malone, R., and Liu, M.: A multidimensional model for aerosols: description of computational analogs, J. Atmos. Sci., 45, 2123–2144, doi:10.1175/1520-0469(1988)045<2123:ammfad>2.0.co;2, 1988.

Toon, O. B., McKay, C. P., Ackerman, T. P., and Santhanam, K.: Rapid calculation of radiative heating rates and photodissociation rates in inhomogeneous multiple scattering atmospheres, J. Geophys. Res., 94, 16287–16301, doi:10.1029/JD094iD13p16287, 1989.

Walko, R. L., Band, L. E., Baron, J., Kittel, T. G. F., Lammers, R., Lee, T. J., Ojima, D., Pielke, R. A., Taylor, C., Tague, C., Tremback, C. J., and Vidale, P. L.: Coupled

atmosphere-biophysics-hydrology models for environmental modeling, J. Appl. Meteorol., 39, 931–944, doi:10.1175/1520-0450(2000)039<0931:cabhmf>2.0.co;2, 2000.
Wiscombe, W. J.: Improved Mie scattering algorithms, Appl. Optics, 19, 1505–1509, 1980.
Yamasoe, M. A., Kaufman, Y. J., Dubovik, O., Remer, L. A., Holben, B. N., and Artaxo, P.: Retrieval of the real part of the refractive index of smoke particles from Sun/sky measurements during SCAR-B, J. Geophys. Res., 103, 31893–31902, doi:10.1029/98jd01211, 1998.

ACPD
12, 17465–17501, 2012

Table 1. Geographical localization of the experimental sites, dominant biomes and available data.

Site	Lat (°)	Lon (°)	Alt. (m)	Dominant ecosystem[a]	Experimental Data
Balbina	−1.92	−59.48	80.0	Tropical Forest beside the Uatumã river	AOD(L2.0)[c]
Belterra	−2.65	−54.95	70.0	Tropical Forest	AOD(L2.0)[c]
Rio Branco	−9.96	−67.87	212	Tropical forest	Shortwave flux[b](L2.0) AOD (L2.0)[c]
Rebio Jaru	−10.083	−61.93	162	Tropical forest surrounded by pasture	AOD (L2.0)[c]
Abracos Hill	−10.76	−62.36	200	Dominated by pasture areas	Shortwave flux[b](L2.0) AOD (L2.0)[c]
Alta Floresta	−9.87	−56.10	277	Transition: Tropical forest to Cerrado	Shortwave flux[b](L2.0) AOD(L2.0)[c]
Cuiabá	−15.73	−56.02	210	Cerrado	Shortwave flux[b](L2.0) AOD(L1.5)[c]
Santa Cruz	−17.80	−63.18	442	Mosaic of dry forest and savanna	AOD (L2.0)[c]

[a] Based on South America biomes map from Stone et al. (1994).
[b] Pyranometer Kipp & Zonen CM 21.
[c] CIMEL CE318 sunphotometer.

ACPD
12, 17465–17501, 2012

Modeling South America regional smoke plume

N. E. Rosário et al.

Table 2. Statistics from comparison between model-calculated aerosol optical depth (AOD) and AERONET measurements. **(a)** All $AOD_{550\,nm}$ conditions; **(b)** only for $AOD_{550\,nm} \leq 1.0$. Root-mean-square error (RMSE), the mean absolute error (MAE), and the mean bias error.

(a)						
All AOD(550 nm)	All Sites	All Sites (no CB)	RB	AH	AF	CB
N	332	267	83	102	82	65
RMSE	0.48	0.34	0.18	0.26	0.52	0.84
MAE	0.26	0.20	0.12	0.18	0.31	0.50
Bias	0.11	0.07	0.002	0.02	0.21	0.25

(b)						
AOD (550 nm) ≤ 1.0	All Sites	All Sites (no CB)	RB	AH	AF	CB
N	263	219	78	83	58	44
RMSE	0.22	0.17	0.16	0.19	0.16	0.36
MAE	0.15	0.12	0.11	0.13	0.12	0.30
Bias	−0.011	−0.0098	−0.006	−0.020	0.0014	0.018

ACPD
12, 17465–17501, 2012
Modeling South America regional smoke plume
N. E. Rosário et al.

Table 3. Statistics from comparison between model-calculated broadband solar irradiance at the surface and pyranometer measurements. Root-mean-square error (RMSE), the mean absolute error (MAE), and the mean bias error are presented.

Solar Irradiance at the surface ($W m^{-2}$)	All Sites	All Sites (AOD $\leq$ 1.0)	All Sites (no CB)	All Sites (no CB and AOD $\leq$ 1.0)
N	260	206	194	156
RMSE ($W m^{-2}$)	45	40	40	31
MAE ($W m^{-2}$)	33	30	29	24
Bias ($W m^{-2}$)	6	11	0.7	7

ACPD
12, 17465–17501, 2012

Table 4. Estimative of smoke aerosol Radiative forcing efficiency (RFE) obtained in the present study and several estimates from previous published studies.

RFE ($W\,m^{-2}/AOD_\lambda$)*	Description	Reference
−154 (λ = 550 nm)	Abracos Hill	This work
−163 (λ = 550 nm)	Rio Branco	
−163 (λ = 550 nm)	Alta Floresta	
−158 (λ = 550 nm)	Southern of the Amazon Basin (Model)	
−141 (λ = 550 nm)	Southern of the Amazon Basin (Empirical)	
−187 (λ = 550 nm)	Cerrado ecosystem	
−145 (λ = 500 nm)	Southern of the Amazon Basin	Schafer et al. (2002)
−210 (λ = 500 nm)	Africa Savanna	Schafer et al. (2002)
−148 ± 44 (λ = 550 nm)	Smoke/dust: Central Africa	Garcia et al. (2011)
−223 ± 39 (λ = 550 nm)	Africa Savanna	Garcia et al. (2011)
−152/ − 194 (λ = 500 nm)	Boulder, Colorado	Stone et al. (2011)

* at noon time

Discussion Paper | Discussion Paper | Discussion Paper | Discussion Paper |

ACPD

12, 17465–17501, 2012

Modeling South America regional smoke plume

N. E. Rosário et al.

Title Page
Abstract Introduction
Conclusions References
Tables Figures
◀◀ ▶▶
◀ ▶
Back Close
Full Screen / Esc
Printer-friendly Version
Interactive Discussion

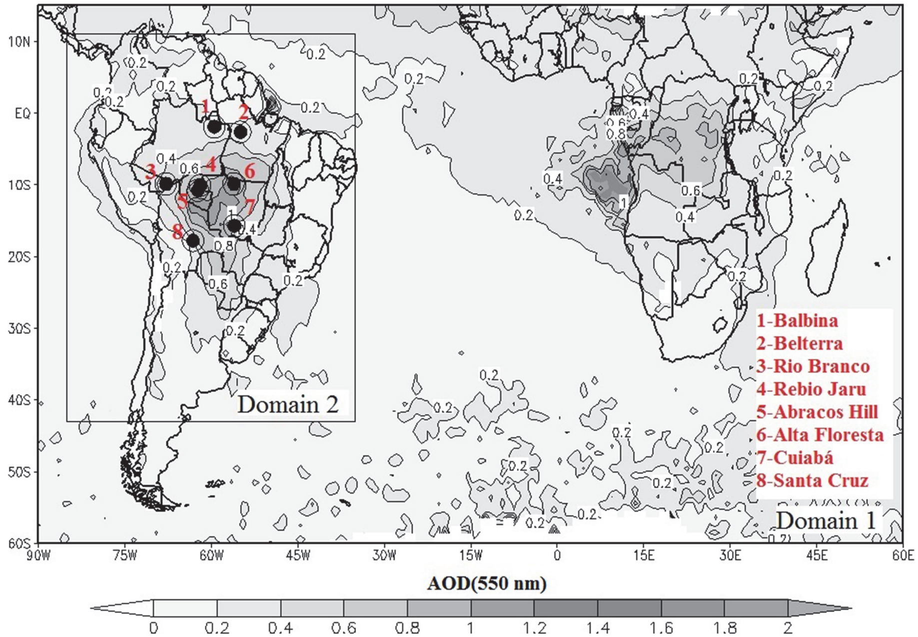

Fig. 1. Geographical localization of experimental sites analyzed depicted along the mean field of aerosol optical (AOD) depth at 550 nm during 2002 biomass burning season in South America obtained from MODIS aboard of TERRA satellite.

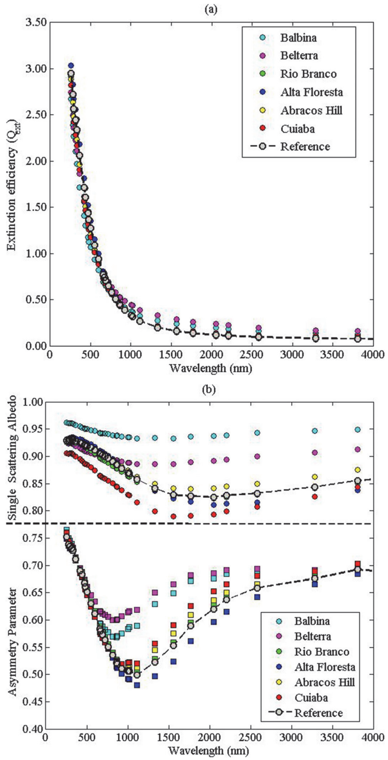

Fig. 2. Optical models describing mean spectral dependence of smoke aerosol optical properties, i.e. **(a)** extinction efficiency, **(b)** single scattering albedo and asymmetry parameter obtained from a Mie code using as input average of size distribution and complex refractive index from each AERONET site. The reference was obtained using averaged microphysical properties from the sites inside the burning areas of the southern part of the Amazon Basin (Rio Branco, Abracos Hill and Alta Floresta).

ACPD
12, 17465–17501, 2012

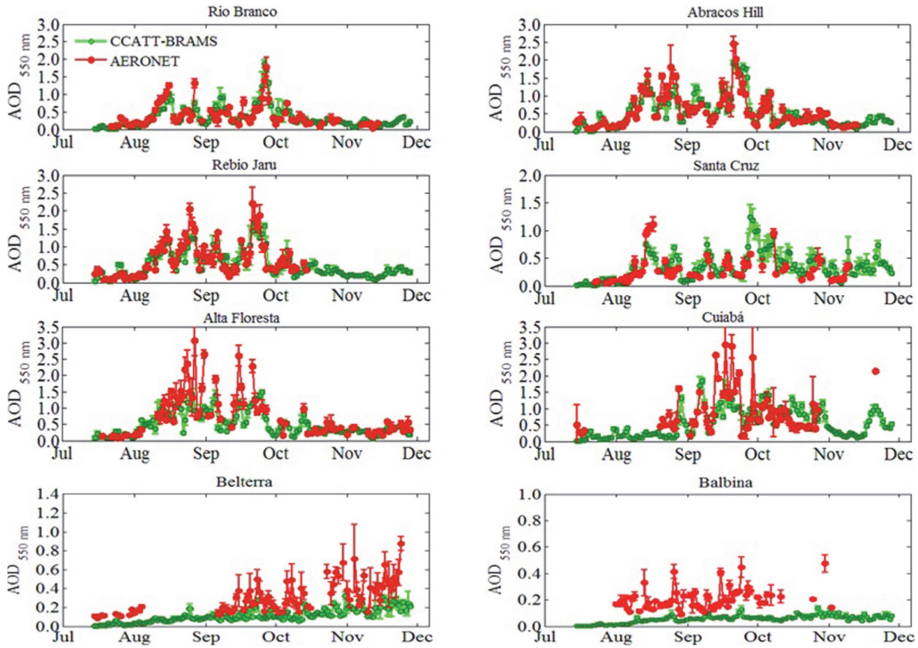

Fig. 3. Intra-seasonal variability of daily mean aerosol optical depth at 550 nm as modeled by CCATT-BRAMS and measured by AERONET sites during the 2002 biomass burning season in South America.

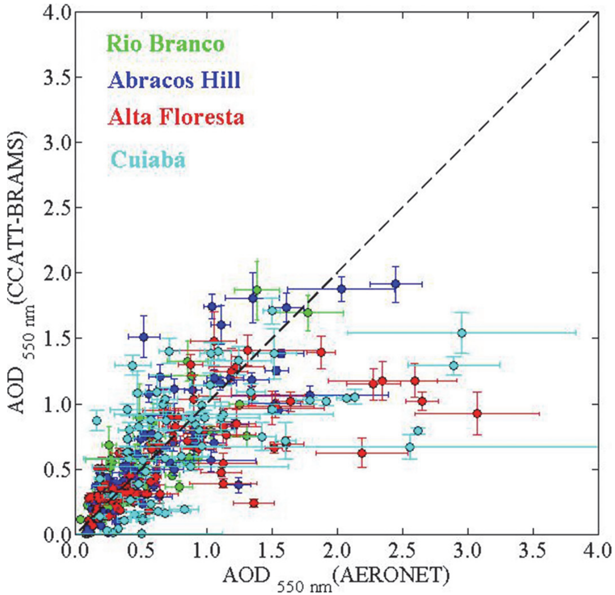

Fig. 4. Modeled (CCATT-BRAMS) versus observed (AERONET) daily mean aerosol optical depth (AOD) at 550 nm over AERONET sites. Bars consist of standard deviation and represent daytime variability of AOD.

ACPD
12, 17465–17501, 2012

Modeling South America regional smoke plume

N. E. Rosário et al.

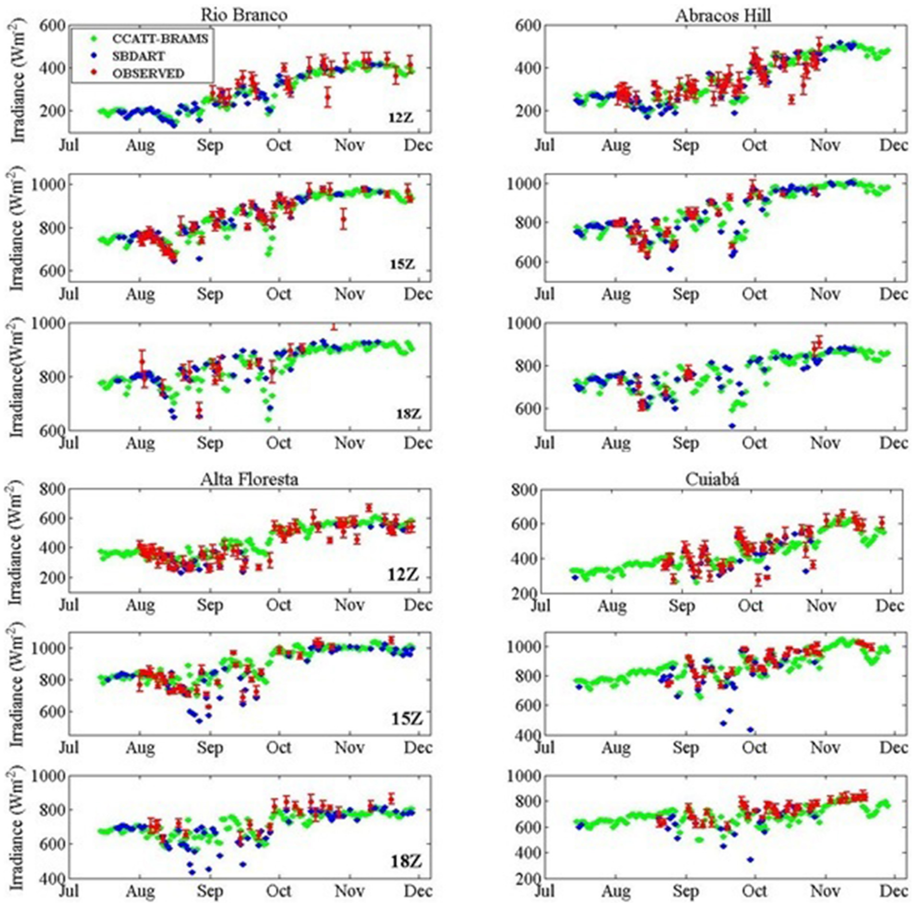

Fig. 5. Modeled (CCATT-BRAMS, SBDART) versus observed downwelling solar irradiance at the surface under cloud-free conditions. SBDART results were obtained using as input aerosol optical depth and column water vapour from AERONET.

ACPD
12, 17465–17501, 2012

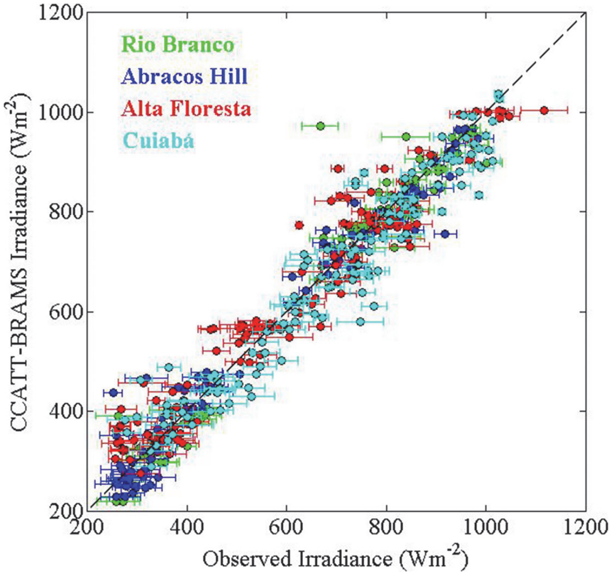

Fig. 6. Model-calculated (CCATT-BRAMS) versus observed downwelling solar radiation at the surface under cloud-free condition at AERONET sites (Rio Branco, Abracos Hill, Alta Floresta and Cuiaba).

ACPD
12, 17465–17501, 2012

Modeling South America regional smoke plume

N. E. Rosário et al.

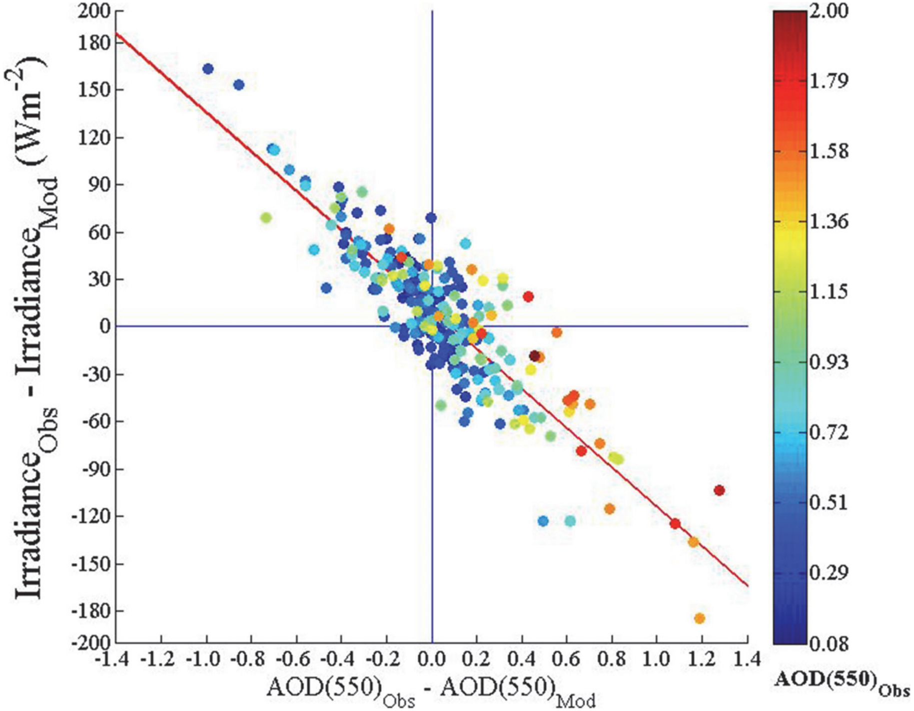

Fig. 7. Difference between downward surface solar irradiance observed and modeled versus difference between aerosol optical depth (AOD) observed and modeled as a function of observed AOD under cloud-free condition.

ACPD
12, 17465–17501, 2012

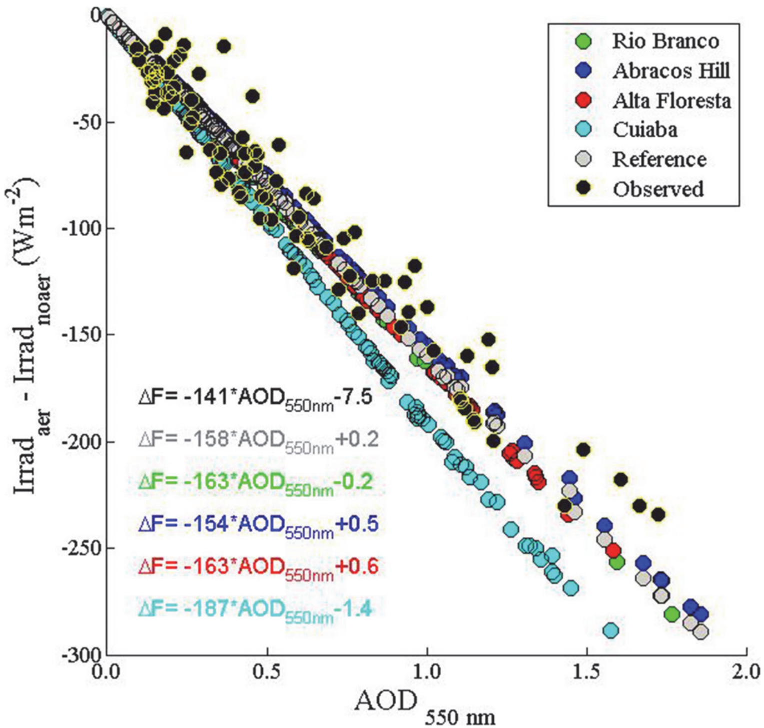

Fig. 8. Linear fitting of aerosol optical depth at 550 nm versus the difference between downward surface solar irradiance considering ($Irrad_{aer}$) and neglecting ($Irrad_{noaer}$) aerosol direct radiative effect. For the observed case $Irrad_{aer}$ consists of pyranometer measurements and $Irrad_{noaer}$ was estimated using SBDART code prescribing water vapour and ozone from observations and turning off aerosol effects. The slopes represent estimates of aerosol radiative forcing efficiency (RFE).

ACPD
12, 17465–17501, 2012

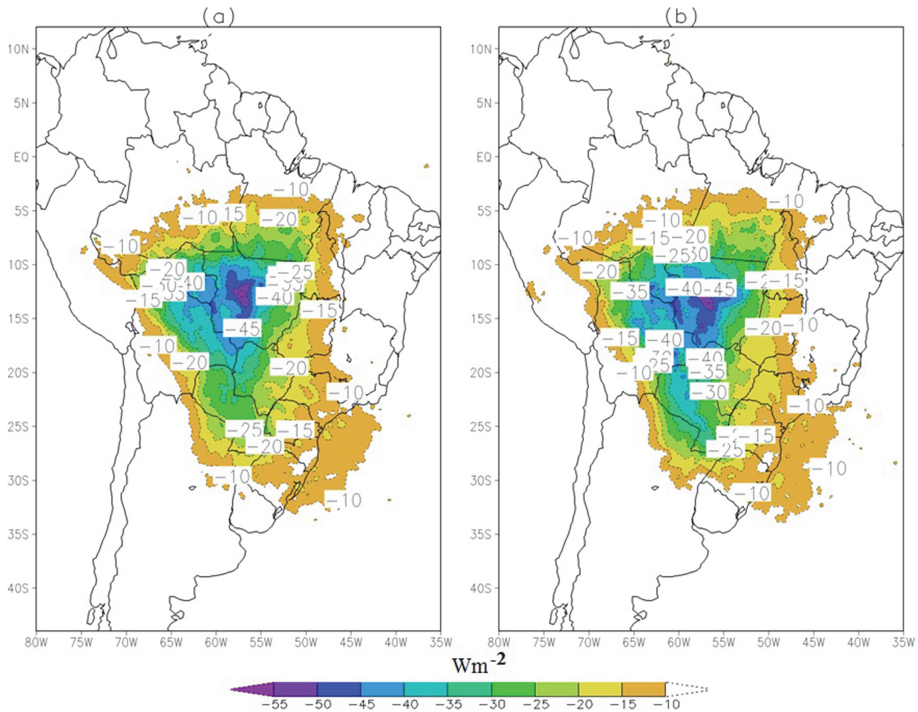

Fig. 9. Biomass burning season mean 24 h surface radiative forcing calculated averaging differences between downward surface solar irradiance including and excluding aerosol direct radiative effect. **(a)** Using a static aerosol optical properties model and **(b)** prescribing spatial varying optical properties models.

ACPD
12, 17465–17501, 2012

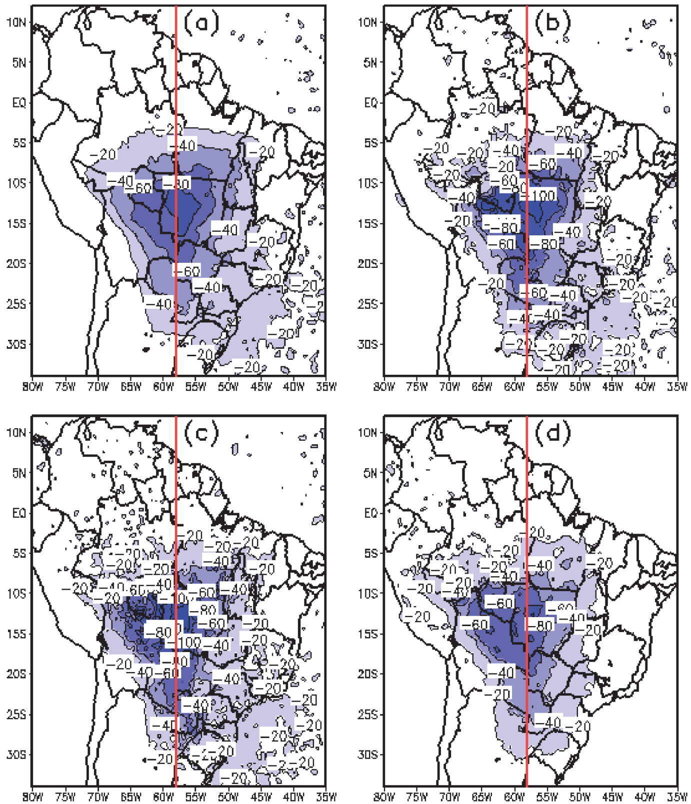

Fig. 10. Biomass burning season mean surface radiative forcing ($W\,m^{-2}$) at specific times calculated averaging differences between downward surface solar irradiance including and excluding aerosol direct radiative effect. **(a)** 12:00 UTC, **(b)** 15:00 UTC, **(c)** 18:00 UTC and **(d)** 21:00 UTC.

ACPD
12, 17465–17501, 2012

Title Page
Abstract | Introduction
Conclusions | References
Tables | Figures
◀| |▶
◀ ▶
Back | Close
Full Screen / Esc
Printer-friendly Version
Interactive Discussion

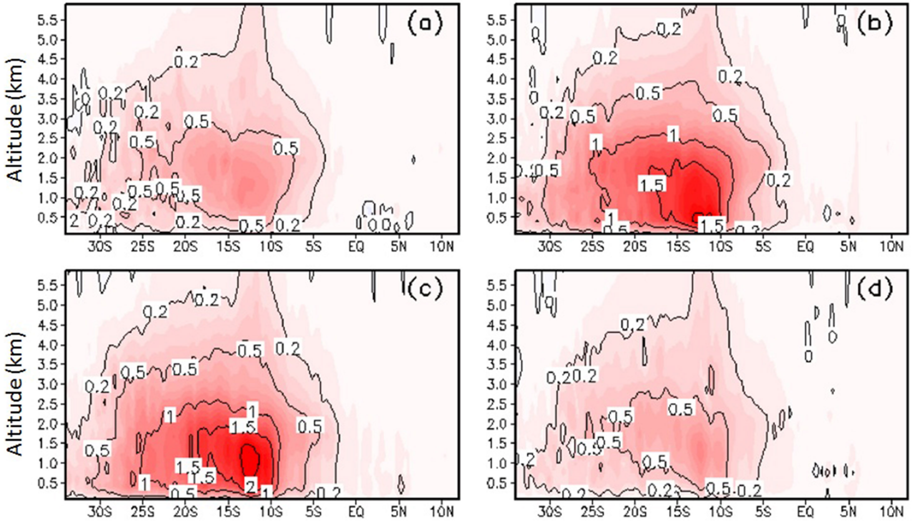

Fig. 11. North-South cross section (red line Fig. 10) average profile of the differences (K day^{-1}) between net radiative heating/cooling rates modeled including and excluding aerosols direct radiative effect over the biomass burning season at **(a)** 12:00 UTC, **(b)** 15:00 UTC, **(c)** 18:00 UTC and **(d)** 21:00 UTC.

ACPD
12, 17465–17501, 2012